A microzonation method based on uniform risk spectra

M. D. TRIFUNAC

Department of Civil Engineering, University of Southern California, University Park, Los Angeles, CA 90089 0242, USA

A method for seismic microzonation of a large metropolitan area is examined. It utilizes information on the location of active faults and their relative levels of seismicity, the three-dimensional source to station geometry, the frequency dependent attenuation, the effects of local amplification of wave amplitudes in terms of the depth of sedimentary deposits beneath the site, and the scaling in terms of earthquake magnitude.

The method presented here does not require any new or difficult steps to gather data, when compared to other microzonation procedures employed in the United States or abroad. The advantage of the method lies in its ability to properly balance different contributing factors to the seismic risk at a point, in time, space and frequency of strong ground shaking.

INTRODUCTION

The seismic zonation maps, usually presented on a scale which only distinguishes areas as large as states or countries, are intended to show the overall distribution of seismic risk. The quantity plotted in such maps may represent a coefficient for use in seismic resistant design[26], maximum intensity of shaking[1,25], or some amplitude of the expected future strong ground motion[8]. Typically, such maps will only include the overall patterns of the geographical distribution of seismicity and may reflect the presence of only some major fault systems or of large seismically active zones. Most seismic design codes include such maps[11] and show the zones requiring different lateral force coefficients.

The characteristics of strong earthquake ground shaking at a point, however, also depend on numerous soil and geological features surrounding the site, as well as on the distribution and on the level of activity of the earthquake sources in the area[9]. These may be too detailed to include in typical seismic zoning maps[11], but can be included in and represent the basis for the detailed microzonation maps. The variety of published microzonation maps results from their many different uses in design[1,24], insurance[27], urban design and in the prediction of earthquake induced soil failures and land slides, for example.

A systematic large scale program to develop zonation maps of the entire country, as well as to develop microzonation maps for large cities started in the USSR in the 1930's[1]. Following the publication of the first USSR zoning map in 1937 many researchers there have worked on the development of the microzonation methodology, which today continues to be dominated by the concept of the largest observed intensity and by the local geologic and subsoil conditions at a site[1]. In Japan the early work on microzonation was influenced by the studies of Sezawa and Kanai on the wave propagation through soil layers and by the effort to measure the transfer function properties of each site experimentally, by studying the local amplitudes of microtremors[13]. In various countries of Europe[14], Central and South America[16,21] and in China[20], the zonation and microzonation work closely followed and combined the Russian and the Japanese experience. In the United States, with few exceptions (e.g. Ref. 25) the microzonation work has not attracted many researchers. In 1972 and 1978 international conferences were held, first in Seattle, Washington, and second in San Francisco, California, to promote international exchange of ideas in microzonation. As can be seen from the proceedings of these two conferences the emphasis in the US seems to be directed towards individual basic or applied studies while an integrated approach to microzonation appears to be lacking.

Following Cornell's pioneering work in 1968, on how to integrate the contributions to the seismic risk at a site, the computational capabilities for evaluating seismic risk have been developed to a point[3,4,5,7,17,22] where this approach can be used now for constructing probabilistic microzonation maps. So far this work has been carried out using mainly the peak ground acceleration and the description of seismicity on the scale of the State of California (for example, Refs 15 and 28). Extending this approach to scaling with frequency dependent spectra (directly) offers major and new possibilities for the development of microzonation maps in which many contributing factors can be considered simultaneously and in a balanced way. To illustrate this method and its capabilities in this paper the results of Lee and Trifunac[19] are presented for microzonation maps of a hypothetical metropolitan area with geometry corresponding to that of the Los Angeles basin.

One of the most important assumptions underlying almost any microzonation method is that the local

Paper accepted December 1987. Discussion closes June 1990.

geologic and soil conditions possess some intrinsic wave amplification properties which are independent (or almost independent) of the type and of the direction of seismic waves approaching the site. This is the basis of all experimental work of Kanai[13], who assumes that by measuring the 'predominant period' of each site, through the experimental measurement of the site transfer function, it is possible to evaluate the local amplification effects[2]. It is also assumed, in this work, that the repeated excitations by different earthquakes will continue to be dominated by the local site effects. For this to be so, it is essential that the local site transfer functions should play a major role in modifying the input ground motion[37]. However, this seems to be so only when the local site consists of exceptionally soft soil and alluvium deposits[10], and when the wave excitation arrives from a limited pencil of azimuths. Detailed analysis of the two- and three-dimensional effects of wave propagation shows that the peaks of the transfer function of the local site effects can shift in their 'predominant period' and in amplitude, and can disappear altogether with changing the direction of wave incidence[30,31]. Though there are many examples of the patterns of building damage following many earthquakes, which are clearly a consequence of the variations of the amplitudes of shaking on a very small (microzonation) scale, there are no adequate data to verify experimentally the extent to which such patterns will be repeated during the future strong earthquake shaking.

Theoretical wave propagation studies and the empirical descriptions of the wave amplitudes do lead to a consistent conclusion that those waves will be amplified which propagate from 'hard' to 'soft' material[30,38]. However, this agreement is only in the sense of the mean overall amplitudes and does not involve any detailed description of the spectral amplification or deamplification at given frequencies or at given locations. This observation thus rules out the concept of the predominant period[13], as it has been associated with the depth of the soft soil deposits[23].

The detailed description of the empirical results which describe the dependence of strong earthquake ground motion amplitudes and duration is beyond the scope of this paper. The most recent results and detailed references on many earlier studies can be found in the reports by Trifunac and Lee[34,35]. For the purposes of this work it is sufficient to state that the repeatable site effects are characterized by the amplification of the average wave amplitudes for periods longer than about 0.5 seconds at geologically 'soft' sites[34,35].

In this paper the methodology for computing the uniform risk spectra will not be presented in detail. This methodology was discussed and illustrated previously through many examples[3,4]. Recently this methodology has been refined by Lee and Trifunac[17] but no new basic principles have been added to the original method. Thus, in the following sections, for completeness of the presentation only, a summary of this method is given so that the reader is reminded briefly of the procedures required for computation of URS.

The purpose of this paper is to show how, by repeating the calculation of URS at a discrete grid of points, a map of URS can be constructed, thus leading to a new method for seismic microzonation. By contrasting the procedures and the results presented with the classical methods for microzonation (e.g. Refs 1, 2, 14, 20, 23, 24, 25), the quantitative and the statistically balanced features of the method proposed here will become clear.

Uniform Risk Spectra

The methodology for estimating the uniform risk spectra at a site[3,4,17] involves: (1) Description of the area surrounding the site in terms of all seismic sources, their activity and geometrical extent, (2) Site characteristics in terms of the depth of sedimentary deposits or the site geological classification[32] and (3) Description of attenuation of strong motion amplitudes with distance from the earthquake source[36]. Then the probability $p[S(\omega)]$ that some spectral amplitude will be exceeded at least once in Y years is[3]

$$p[S(\omega)] = 1 - \exp\{-N_E[S(\omega)]\} \tag{1}$$

where $N_E[S(\omega)]$ is the expected number of times that $S(\omega)$ will be exceeded at the site. The recurrence time of a given amplitude $S(\omega)$ is

$$T[S(\omega)] = N_E[S(\omega)]^{-1} \tag{2}$$

where the time unit is Y years (in all examples in this paper $Y = 50$ years). The above equation (2) then gives the recurrence time of $S(\omega)$. Taking the logarithm of equation (1) gives

$$N_E[S(\omega)] = -\ln\{1 - p[S(\omega)]\} \tag{3}$$

Since, for this discussion, a Poisson sequence of earthquakes in time has been assumed, equation (3) can be used to compute the probabilities of exceeding $S(\omega)$ during another observation period of Y years.

In this paper the examples of microzonation of a metropolitan area are presented assuming that all sources contributing to the risk are represented by a Poissonian sequence in time. However, the computer program which has been employed for all calculations[17], is also capable of considering a combination of Poissonian sources in time with events which will occur with certainty. For example, if a reliable prediction is made that an earthquake of certain magnitude will occur at one of the sources in the model, that source can be assigned the Poissonian sequence plus this deterministic sequence (e.g. main shock and its aftershocks) and the resulting Uniform Risk Spectra can be computed. For examples in this paper such cases have not been considered. Clearly, when final microzonation maps are developed for a region for a period of Y years, and when at some later time an earthquake prediction is made, it is easy to rerun the probabilistic calculations of the microzonation maps to see what is an impact of such a prediction and how and where it may change the previous results based on the Poissonian sequence only, or Poissonian and the predicted sequence, but excluding the prediction just made.

EXAMPLE:

Seismic microzonation of a metropolitan area

To show how the URS methodology could be used to present a microzonation map of a metropolitan area[19], the seismic region and the geometry of the Los Angeles basin in Southern California have been employed.

However, the seismic activity has been chosen arbitrarily. Even though this activity is very similar to the actual one, it *cannot* be taken to represent the author's interpretation of what the seismicity for this area should be. Detailed microzonation of a large metropolitan area like Los Angeles will require very detailed studies of the active faults and of the distribution of all active zones and will call for much more detailed knowledge of the local soil and geologic conditions than what has been adopted for this illustrative example. While many overall features and trends of the 'microzonation maps' presented in this paper will not change much when such detailed information becomes available, the reader is cautioned that this paper presents only an illustration of the methodology and is an example of how the results (Pseudo Relative Velocity (PSV) spectral amplitudes with 5% damping) might vary geographically and with local geologic conditions. From the maps presented here and from the report by Lee and Trifunac[19] one may obtain some idea about the difference of the nature of the PSV spectra at two different sites in the Los Angeles basin, for example, but one cannot take the results to represent reliable estimates of the expected PSV amplitudes for a chosen probability of exceedance.

Figure 1 (modified from Jennings[12]) suggests the distribution of major quaternary faults in Southern California. Figure 2 shows the same region of Southern California and the faults which have been adopted to represent the geometry of earthquake sources in this example. Table 1 presents the seismicity parameters which have been assigned to all sources in Fig. 2

Table 1 Coefficient a in equation (12) and the moment rates per year, $\dot{M}_0$ for 29 faults in Fig. 2. Coefficient a' corresponds to a when M in equation (12) is replaced by site intensity[19]

	FAULT NAME	a (50 YEARS)	a'	MOMENT/YR
1	ELSINORE FAULT - WHITTIER FAULT	3.77	2.69	1.2E+24.
2	CHINO FAULT	1.61	0.55	8.3E+21.
3	ROSE CANYON FAULT	3.28	2.22	3.9E+23.
4	NEWPORT - INGLEWOOD FAULT ZONE	2.92	1.86	1.7E+23.
5	PALOS VERDE FAULT	3.09	2.03	2.5E+23.
6	SAN JACINTO FAULT ZONE	5.05	4.00	2.3E+25.
7	SAN ANDREAS, CAJON TO IMPERIAL VALLEY ON NORTH BRANCH	4.55	3.48	1.5E+25.
8	OAKRIDGE FAULT	2.50	1.44	6.4E+22.
9	SANTA SUSANA FAULT	3.05	2.00	2.3E+23.
10	SIERRA MADRE - CUCAMONGA FAULT ZONE	4.29	3.23	4.0E+24.
11	MALIBU COAST - SANTA MONICA - RAYMOND FAULT SYSTEM	2.50	1.44	6.4E+22.
12	ARROYO PARIDA - SAN CAYETANO FAULT ZONE	2.09	1.03	2.5E+22.
13	SAN ANDREAS FAULT - CAJON PASS TO SAN LUIS OBISPO	5.29	4.23	8.3E+25.
14	BIG PINE FAULT	3.51	2.45	6.6E+23.
15	SANTA YNEZ FAULT - SLIP RATE VERY SPECULATIVE	3.80	2.73	1.3E+24.
16	SAN GREGORIO - HOSGRI FAULT ZONE	4.94	3.88	1.8E+25.
17	PINTO MOUTAIN FAULT	3.25	2.18	3.6E+23.
18	PISGAH - BULLION FAULT	3.67	2.61	9.5E+23.
19	SOUTH DEATH VALLEY FAULT	3.07	2.01	2.4E+23.
20	CALCIO - WEST CALCIO FAULT	3.34	2.29	4.5E+23.
21	CAMP ROCK - EMERSON FAULT ZONE	3.25	2.18	3.6E+23.
22	LOCKHART - LENWOOD FAULT	3.69	2.63	10.0E+23.
23	GARLOCK FAULT	4.68	3.62	9.7E+24.
24	SIERRA NEVADA FAULT	4.03	2.98	2.2E+24.
25	PANAMINT VALLEY FAULT	3.35	2.30	4.6E+23.
26	HELENDALE FAULT	3.32	2.27	4.3E+23.
27	WHITE WOLF FAULT	2.71	1.65	10.4E+22.
28	RINCONADA FAULT	4.14	3.08	2.8E+24.
29	SAN ANDREAS, CAJON TO IMPERIAL VALLEY ON SOUTH BRANCH	4.55	3.48	1.5E+25.

30 DIFFUSE REGION:

MAG	EXPECTED # IN 50 YRS	MMI	EXPECTED # IN 50 YRS
3.5	480.00	4	400.00
4.0	140.00	5	125.00
4.5	42.00	6	25.00
5.0	12.50	7	2.50
5.5	3.65	8	0.00
6.0	1.10	9	0.00
6.5	0.32	10	0.00

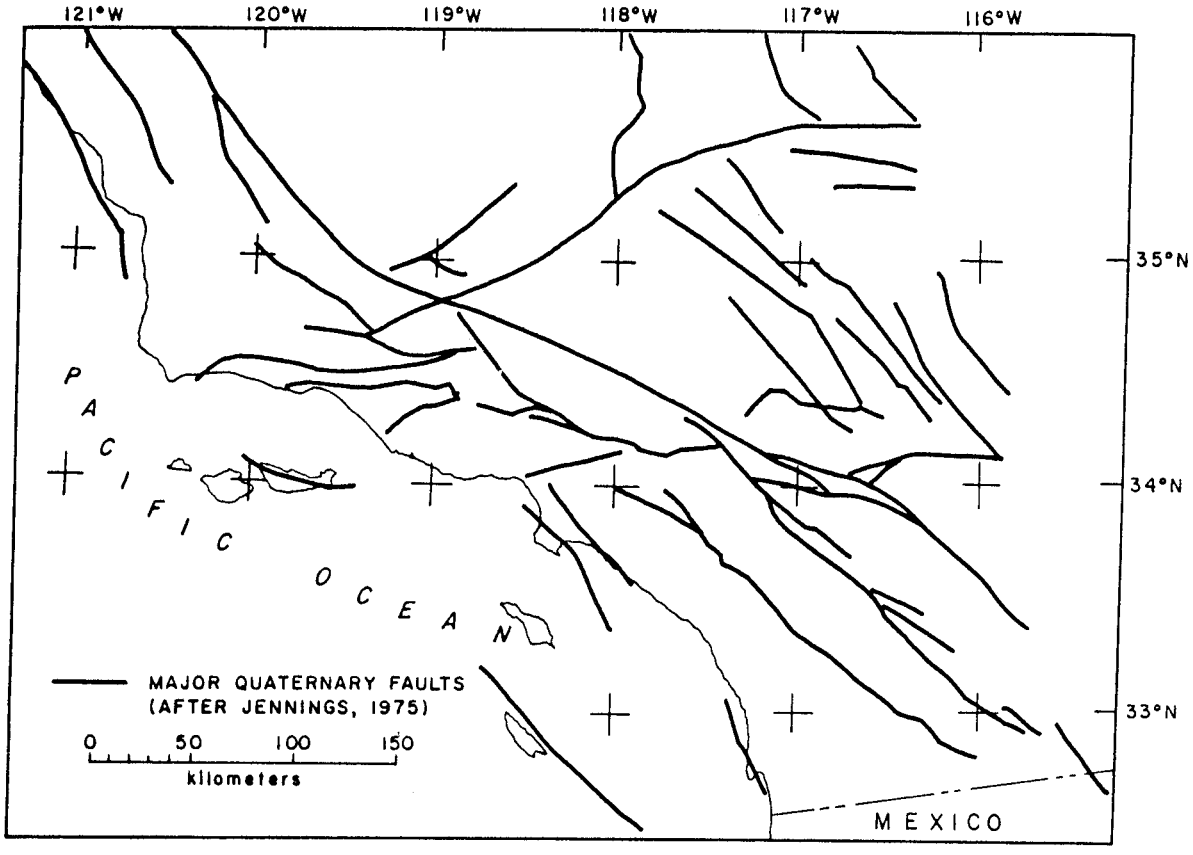
121°W
120°W
119°W
118°W
117°W
116°W
35°N
34°N
33°N
PACIFIC OCEAN
MAJOR QUATERNARY FAULTS
(AFTER JENNINGS, 1975)
0 50 100 150
kilometers
MEXICO

Fig. 1.

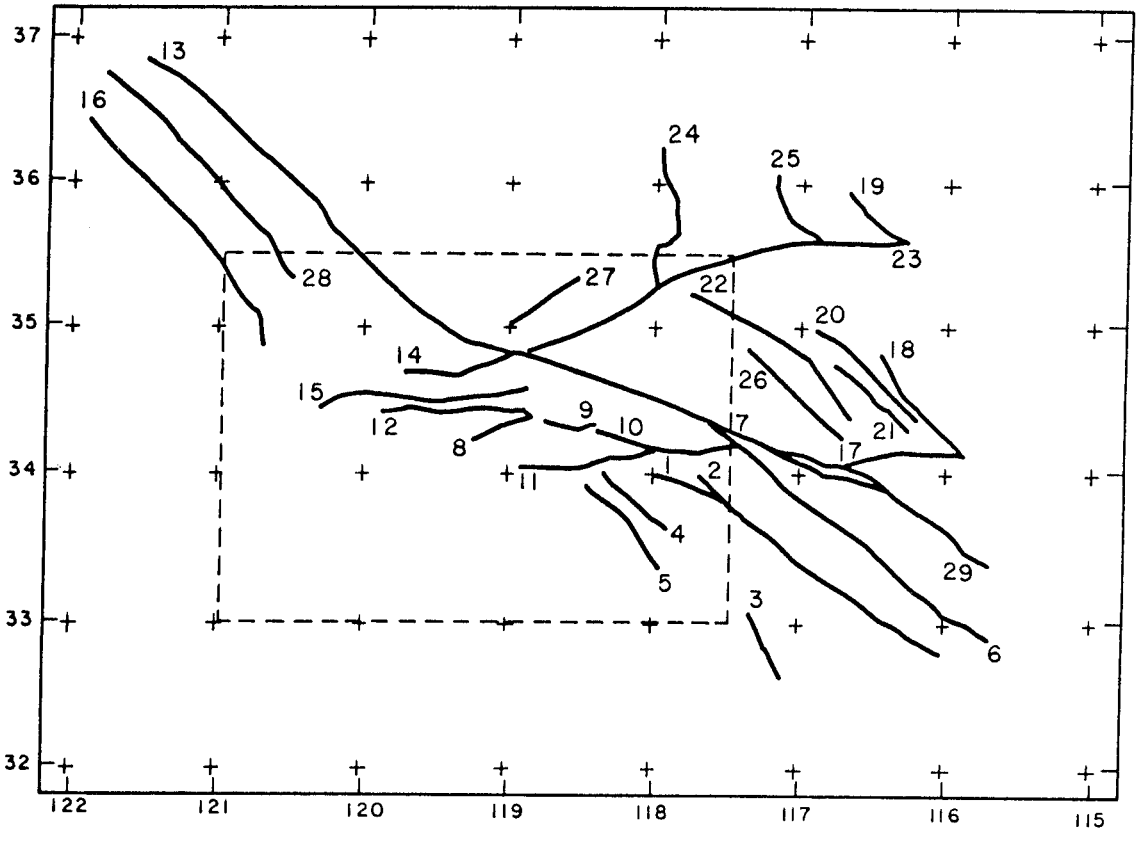
37
36
35
34
33
32
122
121
120
119
118
117
116
115
13
16
24
25
19
23
28
27
22
20
18
14
26
15
12
9
10
7
21
8
17
11
2
4
5
29
3
6

Fig. 2.

(identified by arabic numerals) and which have been used in the computer program NEQRISK[17] to calculate the examples presented in this paper.

There are two sets of inputs for the seismic risk program NEQRISK. The first set of the inputs consists of a description of the seismicity in the region. The second input is the description of the attenuation of seismic waves from the seismic source to the site. Either the magnitude or the MMI models of Trifunac and Lee[35] for the attenuation of the amplitudes of the pseudo-relative velocity spectrum (PSV) at period T can be used. In the model with magnitude scaling,

$$\log_{10} \mathrm{PSV}(T) = M_{<} + \mathscr{A}tt(\Delta, M, T) + b_1(T)M_{<>} + b_2(T)h + b_3(T)v + b_5(T) + b_6(T)M^2_{<>} \quad (4)$$

where T is the period, M is the magnitude of the earthquake, $\mathscr{A}tt(\Delta, M, T)$ the frequency dependent attenuation function developed by Trifunac and Lee[36], $\Delta = \Delta(S, H, R)$ a representative distance from the earthquake source of size S at depth H and at epicentral distance R, h the depth of alluvium, v a component variable set to 0 for horizontal and to 1 for vertical motions and

$$M_{<} = \min(M, M_{\max})$$

$$M_{<>} = \max(M_{\min}, M_{<})$$

where

$$M_{\min} = -b_1(T)/(2b_6(T))$$

and

$$M_{\max} = -(1 + b_1(T))/(2b_6(T)) \quad (5)$$

Using one of the above two sets of inputs, the seismic risk program calculates the PSV amplitudes for a selected set of probabilities of exceedance and a selected set of periods in the range between 0.04 sec–7.50 sec at each site (grid point).

The seismicity of each fault in the region may be described by the occurrence rate of earthquakes on the fault. In selecting this occurrence rate the approach of Anderson and Trifunac[5] has been employed. The seismicity can be estimated from the geological information on the slip of each fault, through the determination of the seismic moment rate, $\dot{M}_0$, which satisfies the following equation,

$$\dot{M}_0 = \int_{-\infty}^{\infty} 10^{\gamma} N(\gamma)\, \mathrm{d}\gamma \quad (6)$$

where $N(\gamma)\,\mathrm{d}\gamma$ is the long term average rate of occurrence of seismic events with moments between $\gamma - \mathrm{d}\gamma/2$ and $\gamma + \mathrm{d}\gamma/2$, where $\gamma = \log_{10} M_0$. $N(\gamma)$ is usually described by

$$N(\gamma) = 10^{c - d\gamma} \quad (7)$$

Assuming that $N(\gamma)$ is zero outside some range $\gamma_{\min} \leqslant \gamma \leqslant \gamma_{\max}$, substituting (7) into (6) and integrating gives

$$\dot{M}_0 = \frac{10^c}{(1-d)\ln 10}\left(10^{(1-d)\gamma_{\max}} - 10^{(1-d)\gamma_{\min}}\right) \quad (8)$$

For earthquakes in Southern California, Thatcher and Hanks[29] give, for M representing the local magnitude,

$$\gamma = 16.0 + 3/2M \quad (9)$$

The frequency of the occurence of earthquakes can be described also directly in terms of magnitude by

$$N(M) = \begin{cases} 10^{a - bM}, & M_{\min} \leqslant M \leqslant M_{\max} \\ 0, & \text{otherwise} \end{cases} \quad (10)$$

with $M_{\min} \leqslant M \leqslant M_{\max}$, the range of allowable magnitudes for the fault, with

$$b = 3/2d$$

and

$$a = c - 16d + \log_{10}(3/2) \quad (11)$$

Here $N(M)dM$ gives the number of events with magnitude between M_1 and M_2. In the present analysis $b = 0.86$. Then from given $\dot{M}_0$, a can be determined through (8) and (11).

To include the uncertainties in the estimation of seismicity through the use of the parameters a, b and $M_{\max}$ in the magnitude model[17], a probability distribution is assumed for

$$\log_{10} N(M) = a - bM \qquad \text{for } M_{\min} \leqslant M \leqslant M_{\max} \quad (12)$$

In the examples of seismic risk analysis in this paper, the $\log_{10} N(M)$ is assumed to follow a triangular distribution (Example b, Section 4.3 of Lee and Trifunac[17]), which is characterized by additional parameters δa and δb. Similarly, $M_{\max}$ can also be described by triangular distribution in the range $M_{\max} \pm \delta M_{\max}$.

Table 1 presents all required information for the seismicity of the 29 faults considered in this study. Column 1 lists the fault numbers, from 1 to 29 (see also Fig. 2). Column 2 gives the 'name' of the fault. Columns 3 and 4 present the coefficients a and a' for calculating $N(M)$ during 50 years. Column 5 gives the adopted moment rate $\dot{M}_0$ per year for each fault. All other coefficients used in the description of seismicity are the same for all the faults, as follows:

$$b = 0.86$$

$$\delta a = 0.42$$

$$\delta b = -0.035$$

$$M_{\max} = \begin{cases} 7.5 \text{ for faults No. 7, 13, 29} \\ 7.0 \text{ for all other faults} \end{cases}$$

$$\delta M_{\max} = 0.5$$

Figure 2 is a plot of the assumed fault sources in the Southern California region that are used in the example for seismic risk analysis in this paper. There are a total of 29 line faults and one region of 'diffused seismicity'[3]. Each

Table 2 Depth of sediments h, in thousands of feet at grid points with 5′ spacing for greater Los Angeles metropolitan area (after Yerkes et al.[39])

	30′	25′	20′	15′	10′	5′	118°00′	55′	50′	45′	40′
20′											
15′		0	0	0	0	0	0	0	0	0	0
10′	6	10	8.5	0	0	1	0	0	0	0	0
5′	0	0	7	9	4	7	10.5	8	2	0	2
34°00′	6	11	20	26	17	18	5	7	5.5	2.5	2
55′	5.5	7.5	11	21	31	25	17	18.5	16.5	5	5
50′	1	5	5.5	11	16	28	23	12	11	10	0
45′		2.5	0	8	10	15.5	18	15.5	8.5	8	5
40′			7.5	4.5	15	13.5	9.5	15	9.5	6	7
35′					9	8	8	6	13.5	8	9
30′										10.5	12

h in thousands of feet

of the 29 line faults is labeled by the corresponding fault number either at the 'beginning' or at the 'end' of the fault. Faults No. 7 and No. 29 have the same beginning and end, as can be seen from the figure. They correspond respectively to the north and south branches of the 'San Andreas' fault from 'Cajon' to 'Imperial Valley'. The diffused region is enclosed by the dashed lines. It ranges from 33° N to 35°30′ N and from 117°30′ W to 121° W. Within this region the earthquakes can occur at any point with uniform probability and with frequency according to the data in Table 1, and for $Y=50$ years.

The scaling equations which relate PSV amplitudes at a given period of motion further require one to specify the 'depth' of sediments beneath the station[35]. Using the maps of Yerkes *et al.*[39] as a general guide, an idealized model of the depth of sediments has been developed. It is presented, in tabular form, in Table 2 for a rectangular

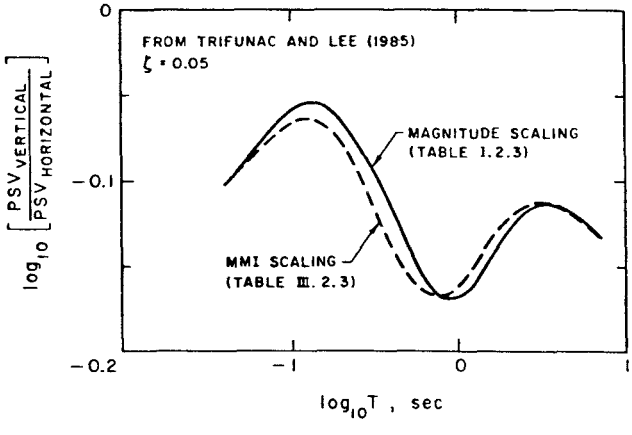

Fig. 3.

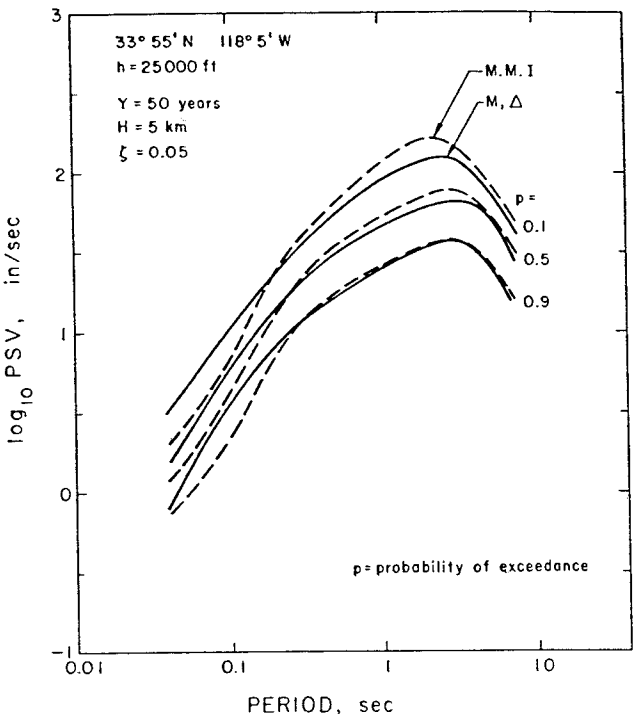

Fig. 4.

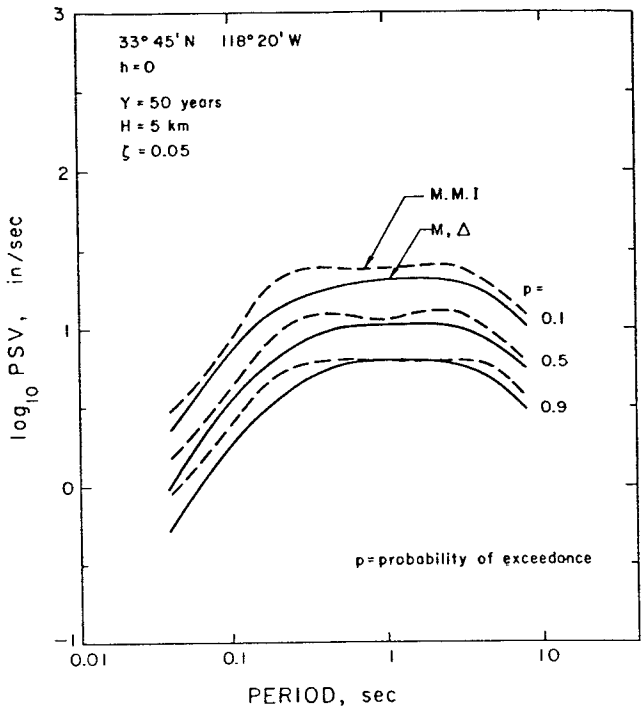

Fig. 5.

mesh with spacing of 5′. It is seen from Table 2 that the depth of sediments ranges from 0 to 31 000 feet (at 118°10′ W and 33°55′ N). From Table 2 the depth at other intermediate coordinates has been interpreted to provide the data for computations at the grid spacing of one minute.

All spectral amplitudes presented in the figures in this paper represent Pseudo Relative Velocity Spectra (PSV) with 5% damping for horizontal ground shaking. The results can be corrected to vertical spectra by multiplying these amplitudes by the scaling factor shown in Fig. 3, plotted versus period T.

The most recent presentation of the spectral scaling equations[35] utilizes the frequency dependent attenuation of strong ground motion[34] and for scaling in terms of the earthquakes magnitude M uses the focal depth H. Since

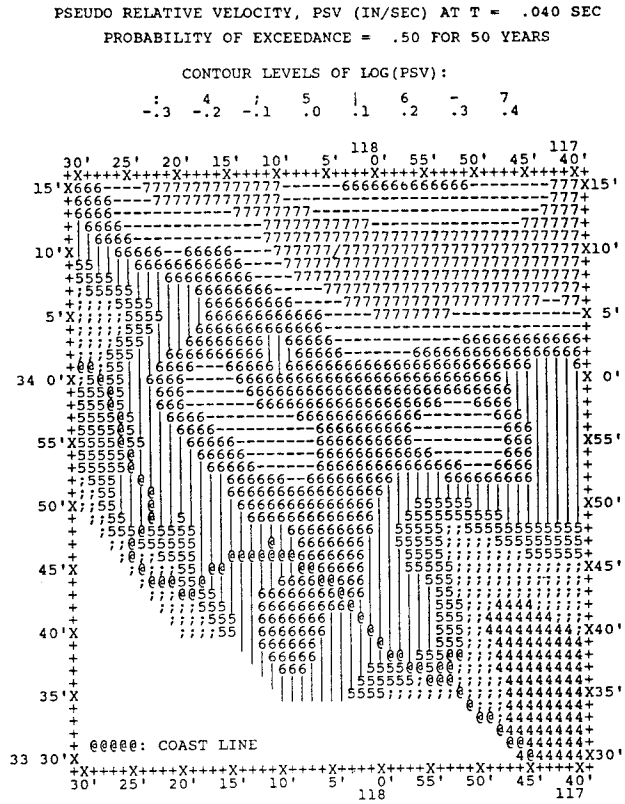

Fig. 6.

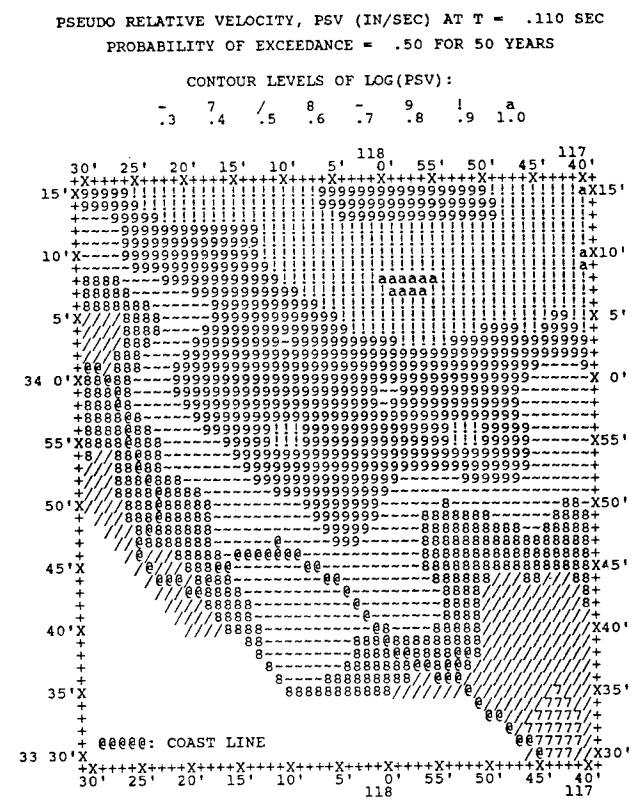

Fig. 7.

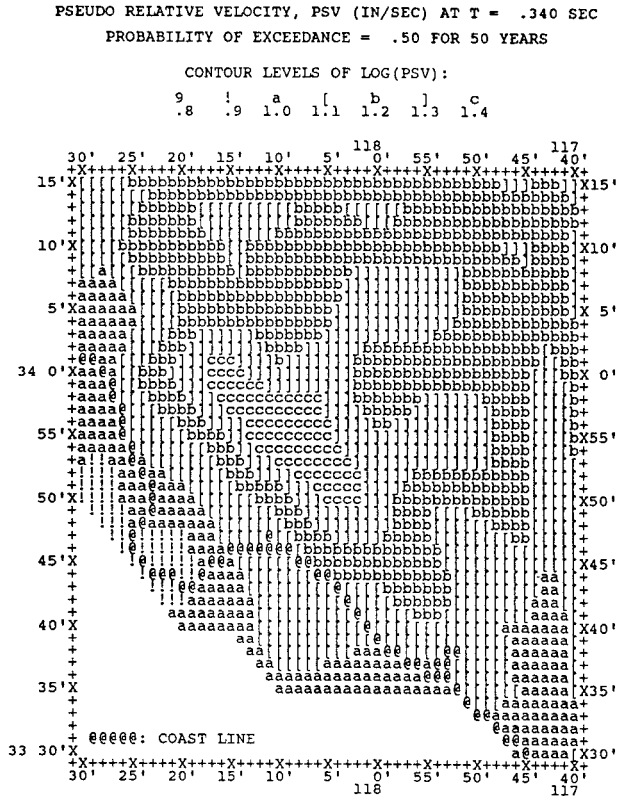

Fig. 8.

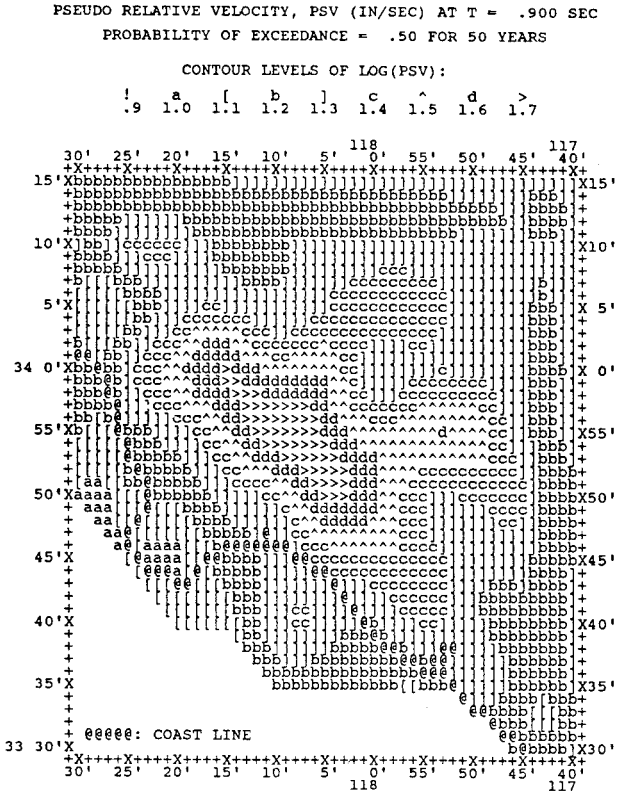

Fig. 9.

most earthquakes in Southern California, which have been recorded by strong motion accelerographs, have H in the range from 0 to about 25 km[18] for simplicity in this paper it has been assumed that all activity occurs at $H = 5$ km. While this assumption should lead to reasonable overall distribution of spectral amplitudes, it must be noted that in localized regions, close to active faults for which H is different from the assumed 5 km, the shape of the Uniform Risk Spectra will be different from what is presented here. This effect is important for high frequency spectral amplitudes only.

Since 1977, when the concept of Uniform Risk Spectra had been proposed[3], we have been developing and improving, in parallel, two independent scaling procedures, one using earthquake magnitude and the other based on the local site intensity (e.g. Ref. 33). In all these analyses we continue to find certain advantages in using the local site intensity. These advantages result from greater simplicity and a smaller number of intermediate computational steps which are involved in scaling with MMI. Though the resulting URS computed with M and with MMI scaling are somewhat different in shape[19] their overall amplitudes agree very well (Figs 4 and 5).

The URS in Figs 6 through 11 have been calculated from a sequence of events at all adopted sources (Table 1 and Fig. 2). In Figs 4 and 5 the two resulting spectra are compared for two sites, one on deep sediments ($h = 25\,000$ feet) at 33°55′ N, 118°5′ W (Fig. 4). In both figures the dashed lines represent the uniform risk PSV spectral amplitudes computed via MMI scaling relations. These have been extracted from the report by Lee and Trifunac[19], and are shown here to illustrate the level of the agreement between URS based on magnitude and MMI scaling equations. The three solid lines in Figs 4 and 5 represent the same spectra, for the probabilities of exceedance $p = 0.90$, 0.50 and 0.10, and computed for the same seismicity model. Comparing the dashed lines for MMI scaling from Lee and Trifunac[19] with the results presented here, it is seen that the two methods of calculation agree remarkably well. For short periods,

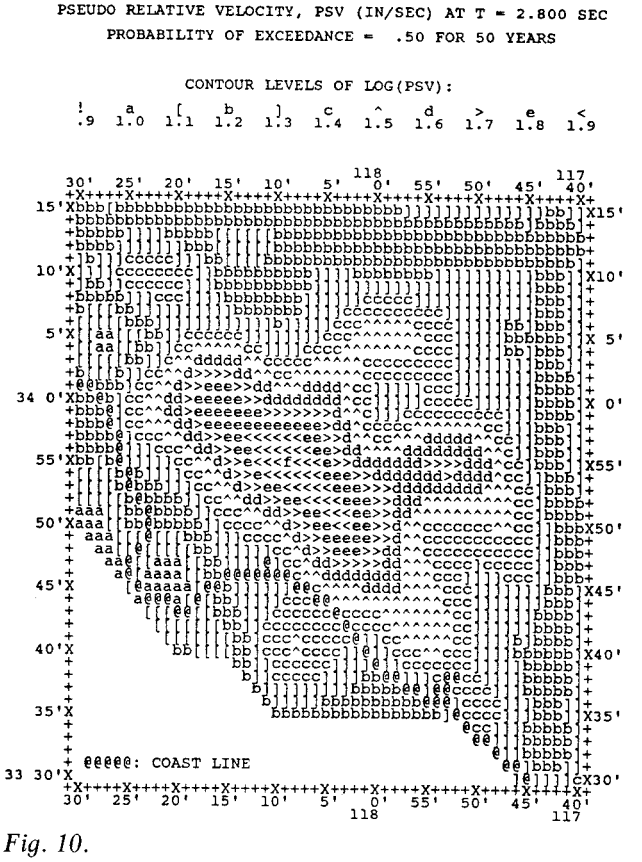

Fig. 10.

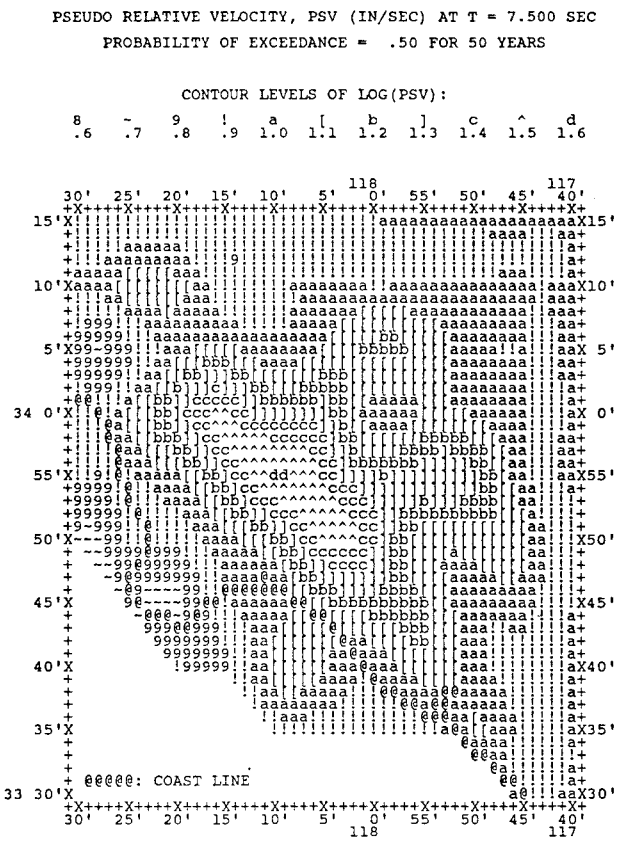

Fig. 11.

shapes of the two estimates are slightly different because the magnitude scaling model assumes the overall average depth of all sources contributing to this URS to be $H = 5$ km, while the scaling in terms of MMI averages over all source depths, by not considering the source depth explicitly[19].

Figures 6 through 11 present examples of the maps of URS for $p = 0.5$ probability of exceedance and for a chosen set of oscillator periods T. The reader can find many such figures for different probabilities of exceedance and for magnitude and MMI scaling in the report by Lee and Trifunac[19]. There are many different ways in which the results such as those illustrated in Figs 6 through 11 can be viewed. One of the most direct ways has already been illustrated in Figs 4 and 5 which have been plotted by interpolating from amplitudes at eleven natural periods at (33°55′ N, 118°5′ W) and (33°45′ N, 118°20′ W) from many figures which are analogous to Figs 6 through 11. By themselves the maps of the type as illustrated in Figs 6 through 11 show the geographical distribution of horizontal PSV amplitudes, for 5% damping, for a given probability of exceedance during 50 years of exposure and for a given oscillator period T. It is seen that by and large the high frequency spectral amplitudes depend on the proximity of the site to 'San Andreas' fault (Fig. 2). At intermediate and long periods the deep sedimentary basin in the central region of the metropolitan area (Table 2) amplifies the longer seismic waves for all probabilities of exceedance.

CONCLUSIONS

The main conclusions of this work can be summarized as follows:

1. The method involving uniform risk spectra[3,17,19] can be used to construct maps of spectral amplitudes with constant probability of being exceeded, at least once in Y years. The method offers excellent means to account for all sources of seismicity and to combine all sources of uncertainty in a uniform and balanced way. It is most efficient in showing the relative significance of different sources, given the different epicentral distances, of the levels of source activity, of the largest magnitude expected at each source, and of the local geologic conditions beneath the site.
2. For the seismicity model selected in the examples presented here, the results are dominated by the expected earthquake occurrence on the 'San Andreas' fault. Its contribution to the risk overshadows all other faults in the metropolitan area.
3. In the central region of the example area, the assumed depth of sediments (Table 2, up to 31 000 feet) significantly amplifies long period ground motion.

REFERENCES

1 Akademia Nauk SSSR, Seismicheskoe Reionirovanie Teritorii SSSR, Izdatelstvo 'Nauka' Moskva 1980
2 Allam, A. An investigation into the nature of microtremors, Ph.D. Thesis, Tokyo Univ., 1969
3 Anderson, J. G. and Trifunac, M. D. Uniform risk functionals for characterization of strong earthquake ground motion, Dept Civil Eng. Report No. 77-02, Univ. Southern Calif., Los Angeles, CA, 1977
4 Anderson, J. G. and Trifunac, M. D. Uniform risk functionals for characterization of strong earthquake ground motion, *Bull. Seism. Soc. Amer.*, 1978, **68**, 205–218
5 Anderson, J. G. and Trifunac, M. D. Application of seismic risk procedures to problems in microzonation, Proc. Second Int. Conf. on Microzonation, Vol I, 559–569, San Francisco, CA, 1978
6 Cornell, C. A. Engineering seismic risk analysis, *Bull. Seism. Soc. Amer.*, 1968, **58**, 1583–1606
7 Der Kiureghian, A. and Ang,, A. H.-S. A line source model for seismic risk analysis, *Struct. Res. Series No. 419*, Univ. Illinois, Urbana, Illinois, 1975
8 Goto, H. and Kameda, H. Statistical reference of the future earthquake ground motion, 4th World Conf. Earthquake Engineering, Santiago, Chile, A-1, 39–54
9 Gaus, M. P. and Sherif, M. A. Zonation and microzonation, in Proc. Microzonation Conference, Seattle, Washington, 1972, **I**, 3–7
10 Herrera, I. and Rosenblueth, E. Response spectra in stratified soil, Proc. Third World Conf. Earthquake Eng., 1965, **1**, 44–60
11 International Association for Earthquake Engineering, Earthquake Resistant Regulations, a World List – 1984
12 Jennings, C. W. Fault Map of California, California Division of Mines and Geology, Sacramento, CA, 1975
13 Kanai, F. Engineering Seismology, Univ. Tokyo Press, Tokyo, Japan, 1983
14 Karnik, V. Microzoning programme within the UNDP–UNESCO survey of the seismicity of the Balkan region, Proc. Microzontaion Conference, Seattle, Washington, 1972, **I**, 213–215
15 Kiremidjian, A. S. Probabilistic hazard mapping in development of site dependent seismic load parameters, Ph.D. Thesis, Stanford Univ., 1977
16 Kuroiwa, J., Deza, E., Jaén, H. and Kogan, J. Microzonation methods and techniques used in Peru, Proc. Second International Conf. on Microzonation, 1973, **I**, 341–352, San Francisco, CA
17 Lee, V. W. and Trifunac, M. D. Uniform risk spectra of strong earthquake ground motion, Dept Civil Eng. Report No. 85-05, Univ. Southern Calif., Los Angeles, CA, 1985
18 Lee, V. W. and Trifunac, M. D. Strong earthquake ground motion data in EQINFOS: Part 1, Dept Civil Eng. Report No. 87-01, Univ. Southern Calif., Los Angeles, CA, 1987
19 Lee, V. W. and Trifunac, M. D. Microzonation of a metropolitan area, Dept of Civil Eng. Report No. 87-02, Univ. Southern Calif., Los Angeles, CA, 1987

20 Liao, Z. Seismic microzonation in China, Institute of Engineering Mechanics, State Seismological Bureau, Research Report 1–37, 1985

21 Lommnitz, C. Global Tectonics and Earthquake Risk, Elsevier Scientific Publishing Company, Amsterdam, 1974

22 McGuire, Seismic structural response risk analysis, incorporating peak response regressions on earthquake magnitude and distance, R 74-51, Dept Civil Eng. Mass. Inst. of Tech., Cambridge, MA, 1974

23 Medvedev, S. V. Inzenernaja Seizmologija, Akademia Nauk SSR, Institut Fiziki Zemli Imeni O. Smidta, Moskva, 1962

24 Osaki, Y. Japanese microzonation methods, Proc. Microzonation Conf., Seattle, Washington, 1972, **I**, 161–182

25 Richter, C. F. Seismic regionalization, *Bull. Seism. Soc. Amer.*, 1959, **49**, 123–162

26 Roberts, E. B. and Ulrich, F. P. Seismological activities of the U.S. Coast and Geodetic Survey in 1949, *Bull. Seism. Soc. Amer.*, 1951, **41**, 205–220

27 Steinbrugge, K. Earthquake insurance and microzonation, Proc. Microzonation Conference, San Francisco, CA, 1978, **I**, 201–213

28 Tenhaus, P. C. *et al.* Probabilistic estimates of maximum seismic horizontal ground motion on rock in coastal California and the adjacent outer continental shelf, U.S.G.S. Open File Report 80-924, 1980

29 Thatcher, W. and Hanks, T. C. Source parameters of Southern California earthquakes, *J. Geophys. Res.*, 1973,, **78**, 8547–8576

30 Trifunac, M. D. Surface motion on a semi-cylindrical alluvial valley for incident SH waves, *Bull. Seism. Soc. Amer.*, 1971, **61**, 1739–1753

31 Trifunac, M. D. Scattering of plane SH waves by a semi-cylindrical canyon, *Int. J. Earthquake Eng. and Struct. Dyn.*, 1973, **1**, 267–281

32 Trifunac, M. D. and Brady, A. G. On the correlation of seismic intensity scales with the peaks of recorded strong ground motion, *Bull. Seism. Soc. Amer.*, **65**, 139–162

33 Trifunac, M. D. Preliminary empirical model for scaling Fourier amplitude spectra of strong motion acceleration in terms of modificed Mercalli intensity and geologic site conditions, *Int. J. Earthquake Eng. and Structural Dynamics*, 1979, **7**, 63–74

34 Trifunac, M. D. and Lee, V. W. Preliminary empirical model for scaling Fourier amplitude spectra of strong ground acceleration in terms of earthquake magnitude, source to station distance, site intensity and recording site conditions: Second Paper, Dept Civil Eng., Report No. 85-03, Univ. Southern Calif., Los Angeles, CA, 1985

35 Trifunac, M. D. and Lee, V. W. Preliminary empirical model for scaling pseudo relative velocity spectra of strong earthquake acceleration in terms of magnitude, distance, site intensity and recording site conditions, Dept of Civil Eng. Report No 85-04, Univ. Southern Calif., Los Angeles, CA, 1985

36 Trifunac, M. D. and Lee, V. W. Frequency dependent attenuation of strong earthquake ground motion, Dept of Civil Eng. Report No. 85-02, Univ. of Southern Calif., Los Angeles, CA, 1985

37 Udwadia, F. E. and Trifunac, M. D. Comparison of earthquake and microtremor ground motions in El Centro, California, *Bull. Seism. Soc. Amer.*, 1973, **63**(4), 1227–1253

38 Wong, H. L. and Trifunac, M. D. Surface motion of a semi-elliptical alluvial valley for incident plane SH-saves, *Bull. Seism. Soc. Amer.*, 1974, **64**, 1389–1408

39 Yerkes, R. F., McCulloh, T. H., Schoellhamer, J. E. and Vedder, J. G. Geology of the Los Angeles Basin, California – an introduction, U.S. Geological Survey Professional Paper 420-A, 1965.